23rd ABCM International Congress of Mechanical Engineering
December 6-11, 2015, Rio de Janeiro, RJ, Brazil

SOLUTION OF THREE DIMENSIONAL STATE ESTIMATION PROBLEM IN RF HYPERTHERMIA USING NANOPARTICLES

Leonardo Antonio Bermeo Varon
Helcio Rangel Barreto Orlande
Federal University of Rio de Janeiro PEM/COPPE-UFRJ, Rio de Janeiro, RJ, 21941-972, Brazil
lebermeo@ufrj.br, helcio@mecanica.coppe.ufrj.br

Guillermo Enrique Eliçabe
University of Mar del Plata, Institute of Materials Science and Technology – INTEMA, J.B. Justo 4302, 7600 Mar del Plata, Argentina
elicabe@fi.mdp.edu.ar

Abstract. *In cancer treatment by radiofrequency (RF) hyperthermia using nanoparticles, there are state variables, which are difficult to observe, quantify or measure, e.g. the heat source, temperature field and electric field. In this treatment the temperature levels are important, as these determine the success of therapy. Thus, the main focus of this paper is the solution to the state estimation problem through the particle filters algorithm for estimating the temperature field. The performance of two particle filters is compared: the sampling importance resampling (SIR) and the Auxiliary Sampling Importance Resampling (ASIR).*

Keywords: *particle filter, RF, nanoparticles, hyperthermia, SIR, ASIR*

1. INTRODUCTION

RF hyperthermia therapy is a cancer treatment type for partial or total elimination of cancer through the heating imposed by electromagnetic waves in frequencies from 3 kHz to 300 GHz (Majchrzak and Paruch 2011a; Lv et al. 2005; Miaskowski and Sawicki 2013; Jamil and Ng 2013; Kurgan and Gas 2015), the high temperature levels are sufficient to kill cells or to make them more susceptible to the effects of radiation and drugs. In that sense, the RF hyperthermia is a treatment used as adjuvant therapy with radiotherapy and chemotherapy to increase efficacy (Wust et al. 2002).

Currently, the combination of RF hyperthermia with tissues loaded by nanoparticles has been studied. In this kind of therapy, nanoparticles introduced into the cancer cells increase the temperature in the tumor tissue at a higher rate than in the normal tissues that does not contain nanoparticles, damaging the tumor only (Majchrzak and Paruch 2011a; Varon et al. 2015; Paruch 2014; Lv et al. 2005).

In the study of RF hyperthermia, Maxwell's equations with frequency dependence are used with the bioheat transfer equation (Pennes 1948). The solution of the mathematical formulation requires the knowledge of several thermophysical properties and other input parameters, which are not widely known and exhibit variability from individual to individual, or even for the same individual under different physiological conditions. Such parameters would need to be estimated indirectly via measurements of other variables in the model or measurements of temperature in the presence of high uncertainty. If such measurements are available, the numerical simulation of the problem containing uncertainties can be envisioned as a state estimation problem (Gordon et al. 1993). In the approach considered here, RF hyperthermia is treated as an inverse problem of state estimation, where the Sampling Importance Resampling (SIR) (Gordon et al. 1993) and Auxiliary Sampling Importance Resampling (ASIR) (Pitt and Shephard 1999) algorithms are applied, with minimally invasive measurements, aimed at better predicting the temperature field in tumor and healthy tissues in order to enhance this cancer treatment and reduce damages to the healthy cells. Nanoparticles of iron oxide (Fe_3O_4) are loaded in the tumor region. A 3D domain is used in the analysis. The forward problem, using the coupled Maxwell's and Pennes' equations, is solved with *Comsol Multiphysics® 5.0* and the solution of inverse problem is coded in *Matlab Mathworks 2012b*.

2. STATE ESTIMATION PROBLEM

In the state estimation problem, consider a model for the evolution of the vector **x** in the following form (Arulampalam et al. 2002):

$$\mathbf{x}_k = \mathbf{f}_k(\mathbf{x}_{k-1}, \mathbf{v}_{k-1}) \tag{1}$$

where the subscript k = 1, 2, . . ., denotes a time instant t_k in a dynamic problem. The vector $\mathbf{x} \in R^{n_x}$ is called the state vector and contains the variables to be dynamically estimated. This vector advances in accordance with the state evolution model given by Eq. (1), where $\mathbf{f}_k$ is a general function of the state variables $\mathbf{x}$ and of the state noise vector $\mathbf{v} \in R^{n_v}$ (Ristic et al. 2004; Arulampalam et al. 2002).

The measurements, $\mathbf{z}_k \in R^{n_z}$, are available at t_k, k = 1, 2, ..., and are related to the state variables $\mathbf{x}_k$ through the general function $\mathbf{h}_k$, the observation model:

$$\mathbf{z}_k = \mathbf{h}_k(\mathbf{x}_k, \mathbf{n}_k) \tag{2}$$

where $\mathbf{n} \in R^D$ is the measurement noise.

The state estimation problem aims at obtaining information about $\mathbf{x}_k$ based on the state evolution model, Eq. (1) and measurement model, Eq. (2) (Kaipio and Somersalo 2004; Arulampalam et al. 2002; Maybeck 1979). The evolution-observation models are based on the following assumptions (Kaipio and Somersalo 2004; Maybeck 1979):

i. The sequence $\mathbf{x}_k$ for k = 1, 2, ..., is a Markovian process, that is,

$$\pi(\mathbf{x}_k|\mathbf{x}_0, \mathbf{x}_1, \ldots, \mathbf{x}_{k-1}) = \pi(\mathbf{x}_k|\mathrm{x}_{k-1}) \tag{3}$$

ii. The sequence $\mathbf{z}_k$ for k = 1,2, ..., is a Markovian process with respect to the history of $\mathbf{x}_k$, that is,

$$\pi(\mathbf{z}_k|\mathbf{x}_0, \mathbf{x}_1, \ldots, \mathbf{x}_k) = \pi(\mathbf{z}_k|\mathbf{x}_k) \tag{4}$$

iii. The sequence $\mathbf{x}_k$ depends on the past observations only through its own history, that is,

$$\pi(\mathbf{x}_k|\mathbf{x}_{k-1}, \mathbf{z}_{1:k-1}) = \pi(\mathbf{x}_k|\mathbf{x}_{k-1}) \tag{5}$$

For the evolution-observation models given by Eqs. (1) and (2), the noise vectors are also assumed to be mutually independent and independent of the initial state $\mathbf{x}_0$ (Kaipio and Somersalo 2004).

The filtering problem of state estimation is considered in this paper. By assuming that $\pi(\mathbf{x}_0|\mathbf{z}_0) = \pi(\mathbf{x}_0)$ is available at time t_0, $\pi(\mathbf{x}_k|\mathbf{z}_{1:k})$ is obtained with Bayesian filters in two sequential steps. The state evolution model is used to advance the vector of state variables from time t_{k-1} to time t_k in the prediction step, thus obtaining a prior distribution $\pi(\mathbf{x}_k)$ for the state variables at time t_k. The information provided by the measurements is then adjoined to this prior distribution in the updated step through Bayes' theorem, by using the likelihood function $\pi(\mathbf{z}_k|\mathbf{x}_k)$ (Kaipio and Somersalo 2004; Arulampalam et al. 2002; Maybeck 1979).

In the solution to the state estimation problem, the Particle Filter method is used in this paper. It is a Monte Carlo technique, where the required posterior density function is represented by a set of random samples (particles) with associated weights; the statistics of the posterior distribution is computed based on these samples and weights. The particle filter algorithms generally make use of an importance density, which is a density proposed to represent another one that cannot be computed exactly, that is, the sought posterior density in the present case. Then, samples are drawn from the importance density instead of the actual density (Andrieu and Doucet 2002; Kaipio and Somersalo 2004; Ristic et al. 2004).

For the particles, $\mathbf{x}_{0:k}^i$, with associated weights w_k^i, $i = 0, \ldots, N$ and set of all state variables $\mathbf{x}_{0:k} = \{\mathbf{x}_j, j = 0, 1, \ldots, k\}$ up to t_k, where N is the number of particles. The weights are normalized so that $\sum_{i=1}^{N} w_k^i = 1$. Then, the posterior marginal distribution can be approximated by (Kaipio and Somersalo 2004; Ristic et al. 2004)

$$\pi(\mathbf{x}_k|\mathbf{z}_{1:k}) \approx \sum_{i=1}^{N} w_k^i \delta(\mathbf{x}_k - \mathbf{x}_k^i) \tag{6}$$

with weights computed from $w_k^i \propto w_{k-1}^i \pi(\mathbf{z}_k|\mathbf{x}_k^i)$ (Ristic et al. 2004).

The particle filter commonly present a degeneracy phenomenon, where after a few states all but very few particles have negligible weight (Ristic et al. 2004; Kaipio and Somersalo 2004; Arulampalam et al. 2002). This problem can be overcome with a resampling step in the application of the particle filter. Resampling can be performed if the number of effective particles (particles with large weights) falls below a certain threshold number, or at every instant t_k, such as in the Sampling Importance Resampling (SIR) (Arulampalam et al. 2002; Ristic et al. 2004). The algorithm is presented in Table 1.

In the SIR algorithm, resampling reduces the effects of degeneration, but the particles with larger weights are selected several times, which can result in a sample with many repeated particles, a phenomenon known as sample impoverishment. The undesirable effect is more significant when the state evolution model has low noise (Arulampalam et al. 2002). The Auxiliary Sampling Importance Resampling (ASIR) algorithm of the particle filter introduced by (Pitt and Shephard 1999) reduces sample impoverishment. Table 2 shows the ASIR algorithm.

Table 1. SIR Particle Filter.

FOR $i = 1, \ldots, N$ $\mathbf{x}_k^i$ from the prior density $\pi(\mathbf{x}_k \mid \mathbf{x}_{k-1}^i)$ $w_k^i = \pi(\mathbf{z}_k \mid \mathbf{x}_k^i)$ using the likelihood density END FOR
Calculate the total weight $T_w = \sum_{i=1}^{N} w_k^i$
FOR $i = 1, \ldots, N$ Normalize $w_k^i = T_w^{-1} w_k^i$ END FOR

Resample
FOR $i = 2, \ldots, N$
$c_i = c_{i-1} + w_k^i$, with $c_1 = 0$; cumulative sum of weights (CSW)
END FOR
With $i = 1$ draw a starting point u_1 from the uniform distribution U[0, N^{-1}]
FOR $j = 1, \ldots, N$
Move along the CSW by making $u_j = u_1 + N^{-1}(j-1)$;
WHILE $u_j > c_i$
$i = i + 1$
END WHILE
assign sample $\mathbf{x}_k^j = \mathbf{x}_k^i$
assign weight $w_k^j = N^{-1}$
END FOR

Table 2. ASIR Particle Filter.

FOR $i = 1, \ldots, N$ $\mathbf{x}_k^i$ from the prior density $\pi(\mathbf{x}_k \mid \mathbf{x}_{k-1}^i)$ calcule the expected value $\mu_k^i = \mathrm{E}[\mathbf{x}_k \mid \mathbf{x}_{k-1}^i]$ $w_k^i = \pi(\mathbf{z}_k \mid \mu_k^i) w_{k-1}^i$ using the likelihood density END FOR
Calculate the total weight $T_w = \sum_{i=1}^{N} w_k^i$
FOR $i = 1, \ldots, N$ Normalize $w_k^i = T_w^{-1} w_k^i$ END FOR

Resample
FOR $i = 2, \ldots, N$
$c_i = c_{i-1} + w_k^i$, with $c_1 = 0$; cumulative sum of weights (CSW)
END FOR
with $i = 1$ draw a starting point u_1 from the uniform distribution U[0, N^{-1}]
FOR $j = 1, \ldots, N$
Move along the CSW by making $u_j = u_1 + N^{-1}(j-1)$;
WHILE $u_j > c_i$
$i = i + 1$
END WHILE
assign sample $i^j = i$
END FOR

FOR $j = 1, \ldots, N$ $\mathbf{x}_k^j$ from the prior density $\pi(\mathbf{x}_k \mid \mathbf{x}_{k-1}^{i^j})$ $w_k^j = \frac{\pi(\mathbf{z}_k \mid \mathbf{x}_k^j)}{\pi(\mathbf{z}_k \mid \mu_k^{i^j})}$ using the likelihood density END FOR
Calculate the total weight $T_w = \sum_{i=1}^{N} w_k^i$
FOR $i = 1, \ldots, N$ Normalize $w_k^i = T_w^{-1} w_k^i$ END FOR

3. PHYSICAL PROBLEM AND MATHEMATICAL FORMULATION

The physical problem considered in this paper involves a domain in 3D, consisting of a rectangular parallelepiped (healthy tissue) (Ω_1), containing a sphere (tumor) (Ω_2), as showed in Fig 1. Heating is imposed by RF waves through the electrodes Ω'_1 and Ω'_2, which are maintained at the voltages U and zero, respectively. The remaining surfaces are electrically insulated. Heat generated by RF inside the domain is propagated by conduction and by blood perfusion. The top and bottom surfaces exchange heat by convection with a surrounding medium, while the remaining surfaces of the domain are supposed to be insulated. The whole region is supposed to be initially at the uniform temperature of the blood (37°C).

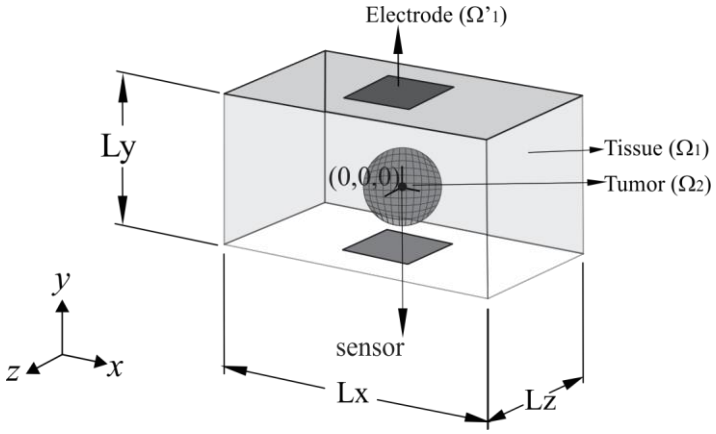

Figure 1. Domain System

The electric potential within the domain can obtained by solving the following Laplace's equation (Cheng 1993) :

$$\nabla\cdot[\varepsilon(x,y,z)\cdot\nabla\varphi(x,y,z)]=0 \qquad x,y,z \in \Omega_1 \cup \Omega_2 \tag{7}$$

where φ is the potential; x,y,z are the Cartesian coordinates; and ε is the permittivity, which varies spatially depending on the tissue and tumor regions.

The interface between the tumor and normal tissues is assumed to have ideal electric contact, that is,

$$\begin{cases} \varphi_1(x,y,z)=\varphi_2(x,y,z) \\ \varepsilon_1 \dfrac{\partial\varphi_1(x,y,z)}{\partial \boldsymbol{n}} = \varepsilon_2 \dfrac{\partial\varphi_2(x,y,z)}{\partial \boldsymbol{n}} \end{cases} \quad \text{at the interface} \tag{8}$$

The boundary conditions for Eq. (7) are given by:

$$\varphi(x,y,z) = U \quad \text{at } \Omega'_1 \tag{9}$$

$$\varphi(x,y,z) = 0 \quad \text{at } \Omega'_2 \tag{10}$$

$$\frac{\partial\varphi(x,y,z)}{\partial n}=0 \qquad \text{at } x,y,z \notin \Omega'_1, \Omega'_2 \tag{11}$$

where U denote the electric potential with respect to ground.

Electric field strength **E** inside the tissue is obtained by Eq. (12) and the intensity of the magnetic field **H** by Eq. (13).

$$\mathbf{E}(x,y,z) = -\nabla\varphi(x,y,z) \tag{12}$$

$$|\mathbf{H}(x,y,z)|=\frac{1}{1+N(\chi)}\frac{|\mathbf{E}(x,y,z)|}{\mu_o \pi f R} \tag{13}$$

where $N(\chi)$=1/3 is the demagnetizing factor of the composite tissue (Andra et al. 1999; Lv et al. 2005), χ is the susceptibility of the magnetic nanoparticles that can be described in terms of complex susceptibility this is $\chi = \chi' +$

$i\chi''$ (Rosensweig 2002; Pankhurst et al. 2003), μ_o is the dielectric constant permeability of free space (μ_o=4π x 10^{-7}T·m·A^{-1}), f is the electromagnetic frequency and R is the radius of magnetic induction loop.

The electric heat source is given by:

$$Q_{e_1}(x,y,z)=\frac{\sigma_1|\mathbf{E}(x,y,z)|^2}{2} \text{ in } \Omega_1 \tag{14}$$

where σ_1 is the electric conductivity of the tissue.

The contribution for the electric heat source resulting from the presence of the magnetic nanoparticles is obtained from (Rosensweig 2002):

$$Q_n=\mu_0\pi f\chi''|\mathbf{H}(x,y,z)|^2 \tag{15}$$

The heat source in tumor due to induction of magnetics nanoparticles by electromagnetic frequency can be calculated by (Andra et al. 1999):

$$Q_{e_2}(x,y,z)=(1-\theta)\frac{\sigma_2|\mathbf{E}(x,y,z)|^2}{2}+\theta\left(\frac{9}{16}\frac{\chi''}{\mu_o\pi fR^2}|\mathbf{E}(x,y,z)|^2\right) \text{ in } \Omega_2 \tag{16}$$

where $\theta=3n\pi r^3/4V$ is the volumetric concentration of nanoparticles, r is the mean radius of the supposedly spherical nanoparticles, n is the number of nanoparticles, V is the volume of the tumor and σ_2 is the electrical conductivity of the tumor tissue embedded with nanoparticles, which can be approximated by an arrangement of the two materials with respective proportions, this is, $1/\sigma_2=(1-\theta)/\sigma_2'+\theta/\sigma_3$ where σ_2' and σ_3 are the electrical conductivity of tumor and nanoparticles, respectively (Majchrzak and Paruch 2011). The permittivity of the tumor tissue embedded with nanoparticles is approximated by $\varepsilon_2 \approx \varepsilon_2'$, where ε_2' is permittivity of the tumor, because the concentration of particles is too small and differences in this parameter for biological tissue and nanoparticles are not evidently large (Lv et al. 2005).

The mathematical formulation for heat transfer is described by Pennes's Equation (Pennes 1948), this equation is denominated the Bioheat transfer.

$$\rho C\frac{\partial T(x,y,z,t)}{\partial t}=\nabla\cdot k\nabla T(x,y,z,t)-\omega_b(x,y,z)\rho_b C_b T(x,y,z,t)+Q(x,y,z,t) \qquad x,y,z\in\Omega_1\cup\Omega_2,\ t>0 \tag{17}$$

where ρ is the density, C is the specific heat, T is the temperature, k is the thermal conductivity, ω_b is the blood perfusion rate, ρ_b is the blood density, C_b is the specific heat of blood and Q is the heat source given by:

$$Q=\omega_b(x,y,z)\rho_b C_b T_b(x,y,z)+Q_m(x,y,z)+Q_e(x,y,z) \tag{18}$$

where T_b is the blood temperature, Q_m is the metabolic heat source and Q_e is the heat source generated by external electromagnetic excitation, Eqs. (14, 16).

The interface tumor and normal tissue is assumed to be in ideal thermal contact, that is:

$$\begin{cases} T_1(x,y,z)=T_2(x,y,z) \\ -k_1\frac{\partial T_1(x,y,z)}{\partial \boldsymbol{n}}=-k_2\frac{\partial T_2(x,y,z)}{\partial \boldsymbol{n}} \end{cases} \quad \text{at the interface} \tag{19}$$

The thermal boundary conditions are given by:

$$\begin{cases} -k\frac{\partial T(x,y,z)}{\partial x}=0, & x=0,L_x,\ t>0 \\ -k\frac{\partial T(x,y,z)}{\partial y}=0, & y=0,L_y,\ t>0 \\ -k\frac{\partial T}{\partial z}(x,y,z)=h_f\left(T(x,y,z)-T_f\right), & z=0,L_z,\ t>0 \end{cases} \tag{20}$$

where h_f is the heat transfer coefficient, T_f is the temperature of the surrounding medium, L_x, L_y and L_z are the domain lengths in the x, y and z directions, respectively.

$$T(x,y,z,0)=T_0(x,y,z),\ x,y,z\in\Omega_1\cup\Omega_2 \tag{21}$$

4. RESULTS AND DISCUSSIONS

A 3D rectangular domain of dimensions L_x = 80 mm, L_y = 40 mm and L_z = 40 mm has been considered, while the tumor is modeled as a sphere of radius 10 mm located in the center of the 3D rectangular domain. The lengths of both electrodes are considered a square with 20 mm sides, so that Ω'_1={-10 mm$\leq x \leq$10 mm, y =20 mm,-10 mm$\leq z \leq$10mm} and Ω'_2 = {-10 mm $\leq x \leq$ 10 mm, y = -20 mm, -10 mm $\leq z \leq$ 10 mm}, and the x, y, z axes are supposed to be located at the tumor center.

For the healthy tissue and the tumor, the following thermal parameters have been assumed: thermal conductivity k_1 = 0.5W/(m.K), k_2 = 0.75W/(m.K), specific heat $C_{b,1,2}$ = 4200 J/(kg.K), density $\rho_{b,1,2}$ = 1000 kg/m^3, perfusion coefficient ω_{b1} = 0.00051/s, ω_{b2} = 0.0021/s, blood temperature T_b = 37°C, the initial temperature T_0 = 37°C, metabolic heat sources Q_{m1} = 4200 W/m^3, Q_{m2} = 42000 W/m^3. For the convective boundary condition we assume T_f = 20°C, and h_f = 45 W/(m^2.K) (Majchrzak and Paruch 2011). For the iron oxide nanoparticles (Fe_3O_4) the following parameters have been considered: thermal conductivity k_3 = 40 W/(m.K), specific heat C_3 = 4000 J/(kg.K), density ρ_3 = 5180 kg/m^3 (Lv et al. 2005), the properties for the tumor embedded with nanoparticles can be approximated by the mixture of the two materials (Andra et al. 1999).

For the electrical parameters in the normal tissue, considering a frequency f = 1 MHz, we used σ_1 = 0.50268 S/m and ε_1 = 1836.4 (Gabriel et al. 1996); while for the tumor tissue, $\sigma_2' = 1.2\sigma_1$ and $\varepsilon_2' = \varepsilon_2 = 1.2\varepsilon_1$ (Majchrzak and Paruch 2011). The electrical properties of the iron oxide nanoparticles were taken as σ_3 = 25000 S/m and χ'' = 18 (Lv et al. 2005). We assumed $n = 10^{14}$ nanoparticles of radius $r = 10^{-8}$ m.

In RF hyperthermia treatment with nanoparticles, the direct problem solution is analyzed with U =15 V applied in the superior electrode and U = 0 V in the inferior electrode, during 900 s, Figure 2 present the temperature fields at t = 900 s at section z = 0. The maximum temperature is 44.25°C in the tumor region, while other regions at lower temperatures.

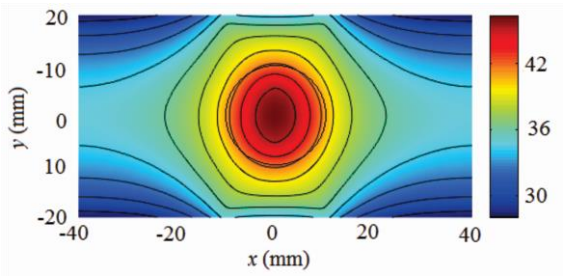

Figure 2. Tissue temperatures at section z = 0

For the solution of the state estimation problem: (i) temperature measurements of one single sensor were assumed available for the inverse analysis, located at the position {x = 0, y = 0, z = 0}. The measurements were generated from the solution of the direct (forward) problem with the parameters specified above. Uncorrelated Gaussian errors with zero mean and standard deviation of 1°C were then added to the solution of the direct problem. The simulated measurements were supposed to be available every 20 s, during 900 s; (ii) Gaussian uncorrelated noise with zero mean and a standard deviation of 1°C were added to the solution of the bioheat transfer problem, which were solved with each sample of the Gaussian distribution of the electrical heat source; (iii) Uncertainties in the electric heat source were considered as a Gaussian random variable with mean and standard deviation of 10% of its exact value; (iv) in the SIR and ASIR filter were used for the solution of the state estimation problem with 100 and 250 particles; (v) were performed 10 repetitions for each algorithm in order to establish the RMS described in Eq. (22) and (vi) is considered the 99% confidence interval for results analysis.

$$\text{RMS}=\sqrt{\frac{1}{M}\sum_{i=1}^{M}[x_s(i)-x_e(i)]^2} \tag{22}$$

where x_s represents the estimated values, x_e represents the exact values and M is the total points.

Table 3 shows the RMS results generated by filter particles for the state estimate. The ASIR filter presents the best performance with respect to the SIR filter, even with a smaller number of particles.

Figure 3 shows the estimated temperature field at the section z = 0 and the t = 900 s, where the estimated maximum temperature for each case was 44.37°C (Fig.3(a)), 43.97°C (Fig.3(b)), 44.52°C (Fig.3(c)) and 44.47°C (Fig.3(d)), which is in good agreement with the exact temperature of 44.25°C.

Figure 4 shows the transient temperature at sensor position {0,0,0}, where the estimated temperature are in better agreement with the exact solution than the measurements. Fig. 5 shows that in the transient temperature at position {0,10,0}, a position where no measurements are available, is observed that the estimated temperature is close to the exact temperature.

Table 3. RMS results

Filter	Number of Particles	$\overline{\text{RMS}}$	Standard Deviation
SIR	100	0.236	0.0207
	250	0.225	0.0196
ASIR	100	0.123	0.0223
	250	0.139	0.0219

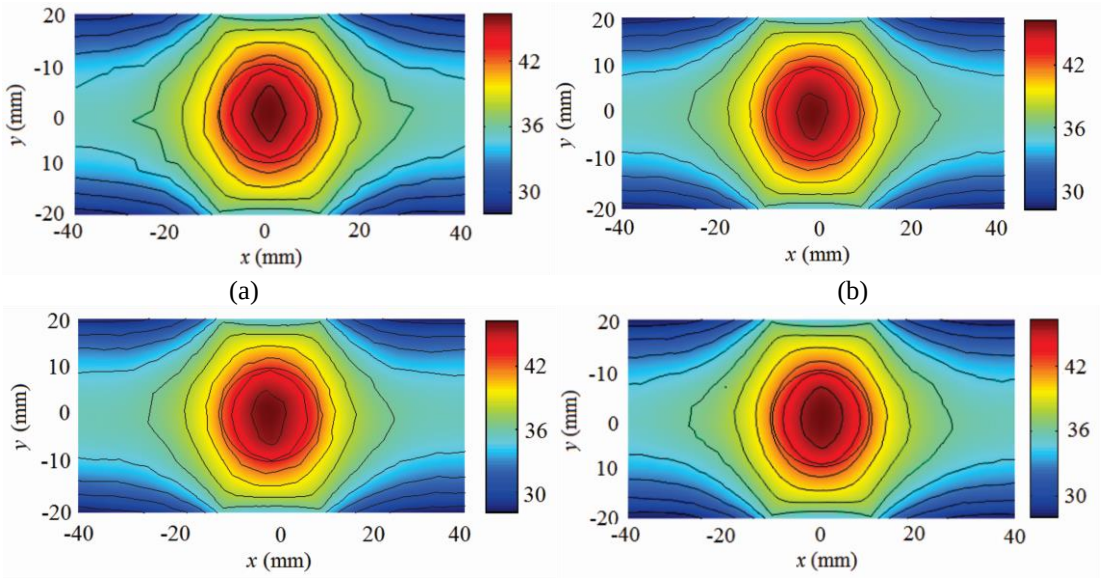

Figure 3. Estimated tissue temperature at section $z = 0$. (a) SIR filter with 100 particles (b) SIR filter with 250 particles (c) ASIR filter with 100 particle (d) ASIR filter with 250 particles

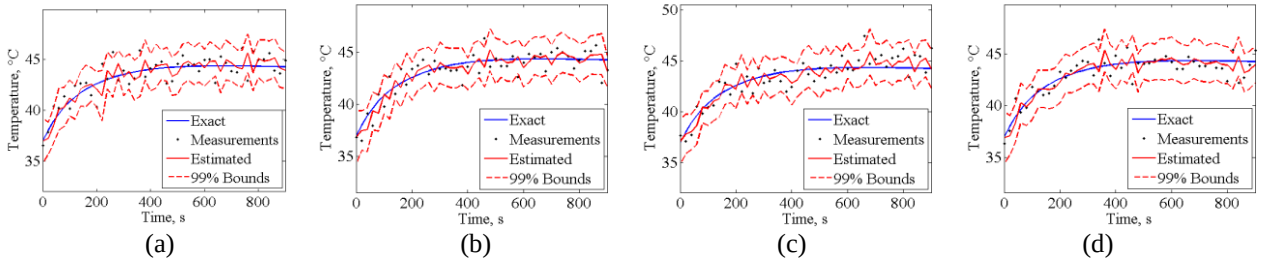

Figure 4. Tissue transient temperature distribution in sensor position $(x,y,z) = (0,0,0)$ (a) SIR filter with 100 particles (b) SIR filter with 250 particles (c) ASIR filter with 100 particle (d) ASIR filter with 250 particles

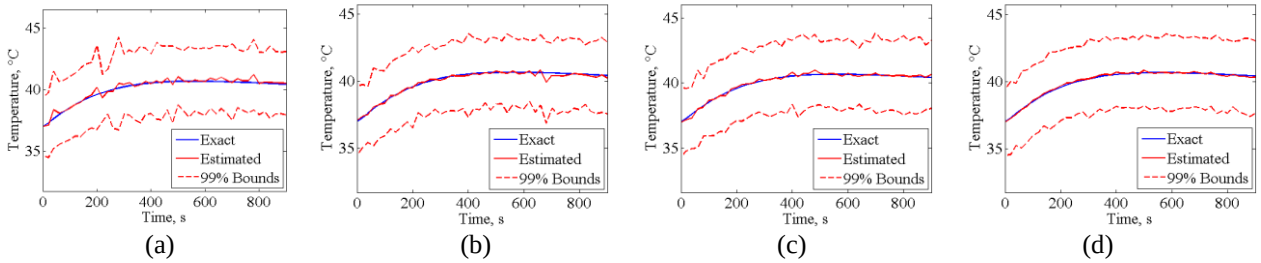

Figure 5. Tissue transient temperature distribution in $(x,y,z) = (0,10,0)$ (a) SIR filter with 100 particles (b) SIR filter with 250 particles (c) ASIR filter with 100 particle (d) ASIR filter with 250 particles

5. CONCLUSIONS

The SIR and ASIR filters are applied to the estimation of the temperature field in RF hyperthermia with nanoparticles, using one single simulated measurement point. The estimate was adequately verified, which involved

large uncertainties in the evolution model and in the simulated measured data. Excellent results were also obtained for the estimated temperature in the whole region, even in locations where no measurements are available. Finally, when the number of particles was increased, the estimates became more accurate and smoother, with excellent agreement with the exact ones.

6. ACKNOWLEDGEMENTS

The authors are thankful for the support provided by CNPq, CAPES and FAPERJ

7. REFERENCES

Andra, W. et al., 1999. "Temperature distribution as function of time around a small spherical heat source of local magnetic hyperthermia". *Journal of Magnetism and Magnetic Materials*, 194, pp.197–203.

Andrieu, C. and Doucet, A., 2002. "Particle filtering for partially observed Gaussian state space models". *Journal of the Royal Statistical Society: Series B Statistical Methodology*, 64(4), pp.827–836.

Arulampalam, M.S. et al., 2002. "A tutorial on particle filters for online nonlinear/non-Gaussian Bayesian tracking". *IEEE Transactions on Signal Processing*, 50(2), pp.174–188.

Cheng, D.K., 1993. *Fundamentals of Engineering Electromagnetics*, United State of America: Addison-Wesley Publishing Company, Inc.

Gabriel, S., Lau, R.W. and Gabriel, C., 1996. "The dielectric properties of biological tissues: III. Parametric models for the dielectric spectrum of tissues". *Physics in medicine and biology*, 41(11), pp.2271–93.

Gordon, N., Salmond, D. and Smith, A.F.M., 1993. "Novel approach to nonlinear and non-Gaussian Bayesian state estimation". *Proc. Inst. Elect. Eng.*, 140, pp.107–113.

Jamil, M. and Ng, E.Y.K., 2013. "To optimize the efficacy of bioheat transfer in capacitive hyperthermia: A physical perspective". *Journal of Thermal Biology*, 38(5), pp.272–279.

Kaipio, J.P. and Somersalo, E., 2004. *Computational and Statistical Methods for Inverse Problems*, Berlin, Heidelberg: Springer.

Kurgan, E. and Gas, P., 2015. "Simulation of the electromagnetic field and temperature distribution in human tissue in RF hyperthermia". *Przeglad Elektrotechniczny*, 1(1), pp.171–174.

Lv, Y.-G., Deng, Z.-S. and Liu, J., 2005. "3-D numerical study on the induced heating effects of embedded micro/nanoparticles on human body subject to external medical electromagnetic field". *IEEE transactions on nanobioscience*, 4(4), pp.284–294.

Majchrzak, E. and Paruch, M., 2011a. "Identification of electromagnetic field parameters assuring the cancer destruction during hyperthermia treatment". *Inverse Problems in Science and Engineering*, 19(1), pp.45–58.

Majchrzak, E. and Paruch, M., 2011b. "Numerical modelling of the cancer destruction during hyperthermia treatment". In *Computer Methods in Mechanics (CMM2011)*. pp. 1–6.

Maybeck, P., 1979. *Stochastic Models, Estimation, and Control.* Academic Press Inc, ed., NY, USA.

Miaskowski, A. and Sawicki, B., 2013. "Magnetic fluid hyperthermia modeling based on phantom measurements and realistic breast model". *IEEE transactions on bio-medical engineering*, 60(7), pp.1806–13.

Pankhurst, Q.A. et al., 2003. Applications of magnetic nanoparticles in biomedicine". *Journal of Physics D: Applied Physics*, 36(13), pp.R167–R181.

Paruch, M., 2014. "Hyperthermia process control induced by the electric field in order to cancer destroying". *Acta of Bioengineering and Biomechanics*, 16(4), pp.123–130.

Pennes, H.H., 1948. "Analysis of tissue and arterial blood temperatures in the resting human forearm". *Journal of applied physiology*, 1(2), pp.93–124.

Pitt, M.K. and Shephard, N., 1999. "Filtering via Simulation: Auxiliary Particle Filters". *Journal of the American Statistical Association*, 94(446), p.590.

Ristic, B., Arulampalam, M.S. and Gordon, N., 2004. *Beyond the Kalman Filter*, Boston, MA: Artech House.

Rosensweig, R.E., 2002. "Heating magnetic fluid with alternating magnetic field". *Journal of Magnetism and Magnetic Materials*, 252, pp.370–374.

Varon, L.A.B., Orlande, H.R.B. and Elicabe, G., 2015. "Estimation of state variables in the hyperthermia therapy of cancer with heating imposed by radiofrequency electromagnetic waves". *International Journal of Thermal Sciencies*, 98, pp.228–236.

Wust, P. et al., 2002. Review Hyperthermia in combined treatment of cancer". *The Lancet Oncology*, 3, pp.487–497.

8. RESPONSIBILITY NOTICE

The authors are the only responsible for the printed material included in this paper.